

Europium Ion Coordination with γ -Carboxyglutamic Acid Containing Ligand Systems

Martha M. Sarasua,^{1a} Mary E. Scott,^{1a} Joseph A. Helpfern,^{1a}
Paul B. W. Ten Kortenaar,^{1a} Norman T. Boggs III,^{1a} Lee G. Pedersen,^{1a}
Karl A. Koehler,^{1b} and Richard G. Hiskey*^{1a}

Contribution from the W. R. Kenan, Jr. Laboratories of Chemistry and the Department of Pathology, The University of North Carolina at Chapel Hill, Chapel Hill, North Carolina 27514. Received September 12, 1979

Abstract: Measurements of europium(III) ion luminescence decay constants, k , were made on solutions of Eu^{3+} complexed to each of the three γ -carboxyglutamic acid containing peptides, Z-Gly-Gla-Gly-OEt (XV), Z-Gla-Ser-OMe (IV), and Z-Gla-Gla-OMe (III), using solvents containing varying ratios of H_2O to D_2O . Plots of the decay constant, k , vs. mole fraction H_2O for all complexes were linear with a constant y intercept. Values of k in 100% H_2O and 100% D_2O were used to construct a scale of N , number of H_2O molecules contained in the Eu^{3+} coordination sphere, from which a value, ΔN , representing the number of H_2O molecules displaced from the Eu^{3+} coordination sphere by ligand complexation, was calculated. ΔN values of 4.1, 3.2, and 4.3 were obtained for complexes of Eu^{3+} with Z-Gly-Gla-Gly-OEt, Z-Gla-Ser-OMe, and Z-Gla-Gla-OMe, respectively, at formal ratios of 2 peptide:1 Eu^{3+} above pH 5.5. Titrations of Eu^{3+} ions with peptide ligands in 100% H_2O were carried out and the luminescence decay constant of Eu^{3+} was measured after each peptide addition and plotted vs. formal ratio of peptide: Eu^{3+} . A nonlinear least-squares analysis of thermodynamic equilibrium models was employed to extract binding constants and complex stoichiometries. Z-Gly-Gla-Gly-OEt (XV) formed predominantly a 2:1 peptide: Eu^{3+} complex with K_1^d (dissociation constant for formation of the 1:1 complex) = $5.9 \mu\text{M}$ and K_2^d (dissociation constant for formation of the 2:1 complex) = $1.5 \mu\text{M}$ and a ΔN of 3.9 indicating a loss of two H_2O molecules from the Eu^{3+} coordination sphere per gla. A pH-dependence study showed no change in ΔN over a pH range from 6.2 to 7.2. Z-Gla-Ser-OMe (IV) formed a 2:1 peptide: Eu^{3+} complex with $K_1^d = 9.1 \mu\text{M}$ and $K_2^d = 20 \mu\text{M}$ and $\Delta N = 3.7$. The pH curve was sigmoidal with a midpoint at pH 4.8. Phe-Leu-Gla-Gla-Leu-OMe formed a 1:1 complex with $K^d = 4.1 \mu\text{M}$ and a ΔN of 4. The pH titration curve was sigmoidal with a midpoint at pH 3.7. Phe-Leu-Gla-Glu-Leu-OMe also formed a 1:1 complex with $K^d = 4.3 \mu\text{M}$ and a smaller ΔN of 2.4. The pH titration curve had a midpoint at pH 4.1. Z-Gla-Gla-OMe formed a 1:2 peptide: Eu^{3+} complex with $K_1^d = 0.6 \mu\text{M}$ and $K_2^d = 1.1 \mu\text{M}$ and ΔN of 3.9. The pH titration curve was sigmoidal with a midpoint at pH 3.7.

Introduction

In 1974 Stenflo et al.^{2a} reported the isolation and characterization of a hitherto unknown amino acid, γ -carboxyglutamic acid (Gla), from a tetrapeptide (residues 6–9) obtained from the amino-terminal region of bovine prothrombin. Independently, Nelsestuen et al.^{2b} also isolated and characterized a Gla-containing dipeptide (residues 33 and 34) from the same protein. The presence of this novel amino acid has been shown to be of primary importance to the proper function of a number of vitamin K dependent plasma proteins involved in blood coagulation.³ Subsequent to isolation from plasma proteins, Gla has also been identified in other systems.⁴

The metal ion binding behavior of Gla in appropriate peptide models is the object of this report. Our particular interest is ultimately the examination of correlations between metal ion binding by this amino acid and metal ion binding by bovine prothrombin, whose activation to the serine protease thrombin is accomplished by factor Xa in the presence of calcium ions, phospholipid, and factor Va.

The calcium ion and phospholipid binding abilities of prothrombin of interest here have been localized to the fragment 1 region of prothrombin (the amino-terminal 156 residues). The presence of ten Gla residues in this region is required for maximal efficiency of phospholipid binding and activation to thrombin.³ The ten Gla residues occur in pairs in the fragment 1 sequence (residues 7/8, 15/17, 20/21, 26/27, and 30/33), suggesting at least five possible sites for metal ion binding. There are also two instances of Gla and serine (Ser) occurring sequentially near one another (residues 24–26 and 33/34). Sequential proximity of ligand atoms is not a requirement for spatial proximity in proteins. Nonetheless, these sequences appear to be appropriate simple models for study in the initial stages of our investigation of metal binding in this system.

The relationship between calcium, magnesium, and lanthanide ion interactions with Gla-containing ligand systems

is a matter of current interest. We have reported^{5,6} initial ⁴³Ca and ²⁵Mg NMR studies of calcium and magnesium ion binding to several synthetic peptides containing Gla-Gla sequences. The present study concerns the use of europium(III) laser-induced luminescence to examine the properties of europium(III) complexes of Gla-containing peptides. The luminescence technique was developed by Horrocks and Sudnick.^{7,8} This important development allows the study of metal-ion binding to biomolecules using direct laser excitation of lanthanide ions. The rate constant for terbium and europium ion luminescence decay in aqueous systems is a sensitive indicator of the number of water molecules in the first coordination sphere of the metal ion since a primary mode of nonradiative decay of the excited ion is through energy transfer to the O–H bonds of water. Because radiative decay is significantly slower than thermal decay, the lifetime of the excited state, and therefore the fraction of the associated energy dissipated through radiative rather than thermal decay, is directly dependent on the number of water molecules adjacent to the ion. Thus we envisaged that the europium(III) luminescence method could be of significant value in the study of metal ions interacting with peptides and proteins containing Gla residues.

Experimental Section

Materials. $\text{EuCl}_3 \cdot 6\text{H}_2\text{O}$ was from Alfa-Ventron Corp. Deuterium oxide was from either Aldrich Chemical Co. or from Merck Sharpe and Dohme Isotopes. All water used was distilled, deionized, and decarbonized. The laser dye 2-(4-biphenyl)-5-phenyl-1,3,4-oxadiazole (PBBO) was obtained from Molelectron. All other reagents used were reagent grade or better.

Sample pH was measured with either a Radiometer Type PHM26c pH meter equipped with a Radiometer GK2322c semimicro electrode or with an Orion Research Model 601A pH meter equipped with an Orion semimicro combination pH electrode. The meters were typically calibrated with two buffers. All readings were uncorrected, including

the readings on deuterium oxide containing solutions. The LC system employed for determination of peptide purity is a Waters Associates instrument, Model M6000A, equipped with a Waters 6000A pump, U6K injector, a Waters Model 450 variable wavelength detector, and a Texas Instrument Co. recorder. A μ -Bondapak C₁₈ column was employed; all samples were eluted with methanol-water (9:1 or 95:5). Detection at 210 nm was generally employed.

Eu³⁺ Binding Experiments. In preparation for Eu³⁺ binding, EuCl₃ and all ligands employed were dried at room temperature in vacuo over phosphorus pentoxide for at least 12 h and then stored in a desiccator prior to use. For the H₂O/D₂O experiments, concentrated stock solutions, typically 10⁻² M, of pure ligand and of pure metal ion were prepared in either 100% H₂O or 100% D₂O. The pHs of the stock solutions were adjusted to the desired values with very small amounts of sodium hydroxide or hydrochloric acid. The final experimental sample solutions of either metal ion plus ligand, in various concentration ratios, or of metal ion alone were prepared by dilution of appropriate amounts of the stock solutions to the desired final concentrations, typically on the order of 1–2 × 10⁻³ M EuCl₃ and/or ligand. These solutions were prepared in solvents containing varying molar ratios of H₂O:D₂O. All D₂O-containing solutions were prepared in a drybox under an argon atmosphere. The Eu³⁺ ion luminescence lifetime at room temperature was then measured for each different solution prepared.

In the ligand titration experiments, samples of 1 mM EuCl₃ were titrated with 10⁻² M stock ligand solutions in 100% H₂O. After each titrant addition the pH of the resulting solution was measured and adjusted to the desired value with small amounts of NaOH or HCl. The europium ion luminescence lifetime at room temperature was measured after each addition of titrant. A titration of free Gla, 1 × 10⁻³ M, pH 7.5, with a 10⁻² M Eu³⁺ solution was carried out in order to provide a basis for comparison of the data obtained by direct metal excitation to that utilizing the energy transfer method reported by Sperling et al.⁹ The reverse titration of 1 × 10⁻³ M Eu³⁺ with a 1 × 10⁻² M free Gla stock solution was also performed to compare the two methods of addition. Equivalent results were obtained by either mode of addition; however, the Gla peptides were titrated by the latter method using peptide as the titrant so that a constant, strong metal ion luminescence signal could be obtained throughout the entire titration. For the pH titrations of Eu³⁺ complexes, each experimental sample consisted of 1 mM EuCl₃ together with the desired formal concentration ratio of ligand:metal. The pH of the solution was then adjusted over a range from pH 1.5 to 8.0 with small amounts of HCl or NaOH. After each pH adjustment the luminescence lifetime of Eu³⁺ was measured. A test of Eu³⁺ binding to ethyl acetate was made to check for the possibility of binding to ester groups used to block the C terminals of the peptides studied. No such binding was observed.

Luminescence Apparatus. An experimental apparatus was constructed for the purpose of measuring lanthanide ion luminescence lifetimes. The excitation source was a Moletron UV 400 nitrogen laser pumping a Moletron DL 200 tunable pulsed dye laser. The laser dye used for direct excitation of Eu³⁺ was PBBO in a 7/3 toluene/ethanol solution at 395 nm. The dye laser energy output using PBBO as the dye was about 70 μ J per 5–10-ns pulse, as measured with a Moletron joulemeter. A pulse repetition rate of 10/s was employed. The experimental Eu³⁺ samples were contained in standard 1-cm quartz fluorimeter cuvettes, placed in a metal thermostable holder and positioned in the laser beam for sample excitation. The Eu³⁺ emission was collected at a 90° angle to the excitation path and then focused onto the entrance slit of a JY H-20-V 0.2-m monochromator (SA Instruments Inc.). The Eu³⁺ emission at 592 nm was collected at the exit slit of the monochromator and focused several millimeters in front of the photocathode on a Hamamatsu R777 photomultiplier tube (PMT). The signal from the PMT was then fed into a Tektronix 7A22 variable bandwidth amplifier of an R7912 Tektronix transient digitizer for dc amplification and digitization.

After digitization the signal was fed into a DEC PDP11/34 computer, where the data was initially signal averaged and then recorded on floppy disks. The luminescence decay curves were regressed directly using a standard weighted linear least-squares analysis for single exponential decays.

Peptide Ligands. *N*-Benzyloxycarbonyl- γ,γ -di-*tert*-butyl-D- γ -carboxyglutamyl- γ,γ -di-*tert*-butyl-D- γ -carboxyglutamic Acid Methyl Ester (I). A suspension of γ,γ -di-*tert*-butyl-D- γ -carboxyglutamic acid¹⁰ (1.82 g, 6 mmol) in dimethylformamide (20 mL) was titrated with a solution of diazomethane in ether until the yellow color per-

sisted. Acetic acid was added to destroy excess diazomethane, and the ether was evaporated in vacuo. *N*-Benzyloxycarbonyl- γ,γ -di-*tert*-butyl-D- γ -carboxyglutamic acid (2.76 g, 6.30 mmol) and 1-hydroxybenzotriazole (0.86 g, 6.35 mmol) were then added, the solution was cooled to 0 °C, and dicyclohexylcarbodiimide (1.31 g, 6.35 mmol) was added. The reaction mixture was stirred for 2 days at 4 °C. The dicyclohexylurea formed was filtered and the filtrate concentrated in vacuo and dissolved in diethyl ether. The ether layer was washed five times with 20% citric acid, once with water, five times with 5% sodium bicarbonate, two times with water, and two times with a saturated solution of sodium chloride. After drying over anhydrous magnesium sulfate, the ether layer was filtered and concentrated in vacuo. The resulting oil was crystallized from ether/pentane to yield 3.47 g (79%) of I, mp 100–101 °C, $[\alpha]_D^{24} +15.7^\circ$ (*c* 0.960, MeOH).

Anal. (C₃₇H₅₆N₂O₁₃) C, N; H: Calcd, 7.66; found, 7.76.

N-Benzyloxycarbonyl- γ,γ -di-*tert*-butyl-L- γ -carboxyglutamyl-L-serine Methyl Ester (II). *N*-Benzyloxycarbonyl- γ,γ -di-*tert*-butyl-L- γ -carboxyglutamic acid¹⁰ (5.0 g, 11.43 mmol) and L-serine methyl ester hydrochloride (1.78 g, 11.43 mmol) were dissolved in acetonitrile (50 mL), and *N*-methylmorpholine (1.28 mL, 11.43 mmol) was added. The solution was then cooled to 0 °C and 1-hydroxybenzotriazole (1.69 g, 12.5 mmol) and dicyclohexylcarbodiimide (2.36 g, 11.43 mmol) were added. The mixture was worked up as described for I. The yield of II was 96% (5.90 g) as a foam, $[\alpha]_D^{23} -7.5^\circ$ (*c* 0.995, MeOH).

Anal. (C₂₆H₃₈N₂O₁₀) C, H, N.

N-Benzyloxycarbonyl-D- γ -carboxyglutamyl-D- γ -carboxyglutamic Acid Methyl Ester (III). The blocked dipeptide I (1.75 g, 2.37 mmol) was stirred for 2 h at room temperature in 90% aqueous trifluoroacetic acid. The trifluoroacetic acid was removed azeotropically with toluene in vacuo. The residue was dissolved in water and washed with diethyl ether. The water layer was lyophilized to dryness to yield 1.23 g (97%) of III as powder, $[\alpha]_D^{22} +18.1^\circ$ (*c* 1.05, water).

Anal. (C₂₁H₂₄N₂O₁₃·3H₂O) C, H, N.

N-Benzyloxycarbonyl-L- γ -carboxyglutamyl-L-serine Methyl Ester (IV). Treatment of II (1.00 g, 1.86 mmol) with trifluoroacetic acid as described for III provided the acid IV as a powder, 0.80 g (99%), $[\alpha]_D^{25} -15.1^\circ$ (*c* 0.955, water).

Anal. (C₁₈H₂₂N₂O₁₀·1/2H₂O) C, N; H: calcd, 5.32; found, 5.35.

N-Benzyloxycarbonyl- γ -*tert*-butyl-L-glutamyl-L-leucine Methyl Ester (V). *N*-Benzyloxycarbonyl- γ -*tert*-butyl-L-glutamic acid dicyclohexylamine salt (0.38 g, 14.0 mmol) and L-leucine methyl ester hydrochloride (2.54 g, 14.0 mmol) were dissolved in dimethylformamide (75 mL). The solution was then cooled to 0 °C, and 1-hydroxybenzotriazole (2.08 g, 15 mmol) and dicyclohexylcarbodiimide (3.17 g, 15 mmol) were added. The mixture was stirred overnight at 4 °C. Subsequent treatment of the reaction mixture was as described for I. The resulting product was a foam and was crystallized by trituration with pentane to yield 5.5 g (85%) of V, mp 39.5–41.0 °C, $[\alpha]_D^{23} -27.5^\circ$ (*c* 1.02, MeOH), homogeneous (LC).

N-Benzyloxycarbonyl- γ,γ -di-*tert*-butyl-L- γ -carboxyglutamyl- γ -*tert*-butyl-L-glutamylleucine Methyl Ester (VI). A sample of V (0.50 g, 1.1 mmol) in acetonitrile (10 mL) was hydrogenated over 10% palladium/carbon (50 mg) at room temperature, the reaction being monitored by TLC. The reaction mixture was filtered directly into a flask containing *N*-benzyloxycarbonyl- γ,γ -di-*tert*-butyl-L- γ -carboxyglutamic acid (0.47 g, 1.1 mmol). This solution was cooled to 0 °C, after which 1-hydroxybenzotriazole (0.16 g, 1.2 mmol) and dicyclohexylcarbodiimide (0.24 g, 1.2 mmol) were added. The reaction mixture was stirred overnight at 4 °C and subsequently treated as described for I. The yield of VI was 80% (0.64 g), mp 101–104 °C, $[\alpha]_D^{23} -26.1^\circ$ (*c* 1.01, MeOH), homogeneous (LC). Amino acid analysis (24-h acid hydrolysis): Glu, 2.00; Leu, 1.00.

Anal. (C₃₈H₅₉N₃O₁₂) C, H; N: calcd, 5.60; found, 5.67.

N-*tert*-Butyloxycarbonyl-L-phenylalanyl-L-leucine Benzyl Ester (VII). To a solution of *p*-toluenesulfonic acid L-leucine benzyl ester (12.6 g, 32 mmol) in dimethylformamide (25 mL) was added *N*-methylmorpholine (3.24 g, 32 mmol). *N*-*tert*-Butyloxycarbonyl-L-phenylalanine (8.48 g, 32 mmol) was dissolved in acetonitrile (25 mL) and added to the reaction mixture, which was then cooled to 0 °C. 1-Hydroxybenzotriazole (5.39 g, 35 mmol) and dicyclohexylcarbodiimide (7.25 g, 35 mmol) were then added. The reaction mixture was stirred at 4 °C for 2 days. Subsequent treatment was as described for I. The yield of VII was 90% (13.48 g), mp 85–85.5 °C, $[\alpha]_D^{22} -27.2^\circ$ (*c* 1.01, MeOH), homogeneous (LC).

Anal. (C₂₇H₃₆N₂O₅) C, H; N: calcd, 5.98; found, 5.94.

***N*-tert-Butyloxycarbonyl-L-phenylalanyl-L-leucine Hydrazide (VIII).** A solution of VII (6.0 g, 12.8 mmol) in methanol (25 mL) was treated with hydrazine monohydrate (1.9 g, 38.4 mmol). The reaction mixture was allowed to stand at room temperature for 5 days. The solvent was removed in vacuo, leaving a white solid residue which was washed with diethyl ether and filtered to yield 3.63 g (72%) of VIII, mp 160–162.5 °C, [α]_D²³ –27.2° (c 1.01, MeOH), homogeneous (LC).

Anal. (C₂₀H₃₂N₄O₄) C, H, N.

***N*-tert-Butyloxycarbonyl-L-phenylalanyl-L-leucyl-γ,γ-di-tert-butyl-L-γ-carboxyglutamyl-γ-tert-butyl-L-glutamyl-L-leucine Methyl Ester (IX).** A sample of VI (0.55 g, 0.75 mmol) in acetonitrile (6 mL) was hydrogenated over 10% palladium/carbon (0.60 g) at room temperature, the reaction being monitored by TLC. The reaction mixture was filtered to remove the catalyst. Solvent was removed from the filtrate in vacuo. The resulting oil was dissolved in a small amount of dimethylformamide and added to an azide coupling mixture prepared as follows. VIII (0.32 g, 0.82 mmol) was dissolved in dimethylformamide (4 mL) and cooled to –15 °C in a CCl₄/dry ice bath. Hydrochloric acid (0.7 mL, 2.46 mmol, 3.5 N in ethyl acetate) and *tert*-butyl nitrite (0.11 mL, 0.98 mmol) were added, and the reaction mixture was allowed to stir for 0.5 h. At the end of that time the reaction mixture was neutralized with *N*-methylmorpholine to pH 7–8. The hydrogenation product, in a small amount of dimethylformamide, was added to this solution, and the reaction mixture was allowed to stir at 4 °C for 2 days. Sodium bicarbonate (5%, ca. 1.5 mL) was then added to destroy any excess azide. The solvent was removed in vacuo, leaving an oily residue. The oil was dissolved in ethyl acetate and successively washed once with water, twice with 5% sodium bicarbonate, once with water, twice with 20% citric acid, once with water, and twice with a saturated sodium chloride solution. After drying over anhydrous magnesium sulfate, the ethyl acetate layer was concentrated in vacuo. The resulting oil was triturated with diisopropyl ether, and the resulting white solid was recrystallized from warm ethyl acetate to yield 0.5 g (68%) of pentapeptide derivative, mp 187–191 °C, [α]_D²⁵ –34.0° (c 0.975, MeOH); homogeneous (LC). Amino acid analysis (24-h acid hydrolysis): Glu, 1.85; Leu, 2.03; Phe, 1.00.

Anal. (C₅₀H₈₁N₅O₁₄) C, H, N.

L-Phenylalanyl-L-leucyl-L-γ-carboxyglutamyl-L-glutamyl-L-leucine Methyl Ester Trifluoroacetate Salt (X). A solution of IX (0.40 g, 0.41 mmol) in 90% aqueous trifluoroacetic acid (15 mL) was stirred for 2 h at room temperature. Excess trifluoroacetic acid was removed azeotropically with toluene in vacuo. The residue was dissolved in water, washed with ethyl acetate, and then lyophilized to a white powder, [α]_D²³ –34.8° (c 1.01, water), homogeneous, electrophoresis, pH 6.4 (9:1:0.04 H₂O/pyridine/AcOH). Amino acid analysis (24-h acid hydrolysis): Glu, 2.00; Leu, 2.02; Phe 0.96.

Anal. (C₃₅H₅₀N₅O₁₄F₃) C; H; calcd, 6.13; found, 6.28. N: calcd, 8.52; found, 8.45.

***N*-Benzyloxycarbonyl-γ,γ-di-tert-butyl-L-γ-carboxyglutamyl-L-leucine Methyl Ester (XI).** A solution of *N*-benzyloxycarbonyl-γ,γ-di-tert-butyl-L-γ-carboxyglutamic acid (1.0 g, 2.28 mmol) and L-leucine methyl ester hydrochloride (0.46 g, 2.50 mmol) in dimethylformamide (15 mL) was treated with *N*-methylmorpholine (0.28 mL, 2.5 mmol) while cooling in an ice bath. 1-Hydroxybenzotriazole (0.34 g, 2.5 mmol) and dicyclohexylcarbodiimide (0.52 g, 2.5 mmol) were then added and the solution was stirred for 2 days at 4 °C. Subsequent treatment of the reaction mixture was as described for I resulting in 1.12 g (87%) of a colorless oil, [α]_D²⁵ –21.96° (c 0.95, MeOH). Amino acid analysis: Glu, 1.00; Leu, 1.08.

Anal. Calcd for C₂₉H₄₄N₂O₉: C, 61.68; H, 7.85; N, 4.96. Found: C, 61.45; H, 7.86; N, 4.92.

***N*-Benzyloxycarbonyl-γ,γ-di-tert-butyl-L-γ-carboxyglutamyl-γ,γ-di-tert-butyl-L-γ-carboxyglutamyl-L-leucine Methyl Ester (XII).** A solution of XI (1.0 g, 1.8 mmol) in acetonitrile (30 mL) was hydrogenated over 10% palladium/carbon (100 mg) at room temperature and followed to completion (3 h) by TLC. The reaction mixture was filtered directly into a flask containing *N*-benzyloxycarbonyl-γ,γ-di-tert-butyl-L-γ-carboxyglutamic acid (0.772 g, 1.8 mmol) while stirring in an ice bath. 1-Hydroxybenzotriazole (0.26 g, 1.95 mmol) and dicyclohexylcarbodiimide (0.40 g, 1.95 mmol) were added and the reaction mixture was stirred overnight at 4 °C. Subsequent treatment of the reaction mixture was as described for I to yield 1.43 g (95%) of XII as a colorless foam, [α]_D²³ –25.8° (c 1.08, methanol), homogeneous (LC). Amino acid analysis: Glu, 2.00; Leu, 1.21.

Anal. Calcd for C₄₃H₆₇N₃O₁₄: C, 60.76; H, 7.94; N, 4.94. Found: C, 60.55; H, 7.91; N, 5.00.

***N*-tert-Butyloxycarbonyl-L-phenylalanyl-L-leucyl-γ,γ-di-tert-butyl-L-γ-carboxyglutamyl-γ,γ-di-tert-butyl-L-γ-carboxyglutamyl-L-leucine Methyl Ester (XIII).** A sample of XII (1.29 g, 1.52 mmol) in acetonitrile (20 mL) was hydrogenated over 10% palladium/carbon (130 mg) at room temperature and followed to completion by TLC. The reaction mixture was filtered to remove the catalyst and the solvent was removed in vacuo. The resulting oil was dissolved in a small amount of dimethylformamide and was added to an azide coupling mixture prepared as follows: 656 mg (1.67 mmol) was dissolved in DMF (4 mL) and cooled to –15 °C (CCl₄/dry ice). Hydrochloric acid (1.47 mL, 3.4 N in ethyl acetate) and *tert*-butyl nitrite (0.24 mL, 2.0 mmol) were added and the reaction mixture was allowed to stir for 0.5 h. At the end of that time the reaction mixture was neutralized with methylmorpholine to pH 7–8. The hydrogenation product, in a small amount of dimethylformamide, was added to this solution and the reaction mixture was stirred at 4 °C for 2 days. Sodium bicarbonate (5%, ca. 3 mL) was then added to destroy any excess azide, and the solvent was then removed in vacuo. The resulting oil was dissolved in ethyl acetate and subsequent treatment was as described for I. The product was recrystallized from warm diisopropyl ether to yield 1.25 g (77%), [α]_D²³ –30.3° (c 0.99, MeOH), mp 153.5 °C, homogeneous (LC). Amino acid analysis: Glu, 2.00; Leu, 2.09; Phe, 0.91.

Anal. Calcd for C₅₅H₈₉N₅O₁₆: C, 61.37; H, 8.33; N, 6.51. Found: C, 61.29; H, 8.39; N, 6.46.

L-Phenylalanyl-L-leucyl-L-γ-carboxyglutamyl-L-γ-carboxyglutamyl-L-leucine Methyl Ester Trifluoroacetate Salt (XIV). A solution of XIII (0.47 g, 0.44 mmol) in 90% aqueous trifluoroacetic acid (14 mL) was stirred for 2.5 h at room temperature. Subsequent treatment of the reaction mixture was as described for X to provide a quantitative yield of XIV, [α]_D²³ –29.10° (c 1.09, MeOH). Amino acid analysis: Glu, 2.00; Leu, 1.92; Phe, 0.92.

Anal. Calcd for C₃₈H₅₁N₅O₁₈F₆: C, 46.58; H, 5.25; N, 7.15. Found: C, 46.65; H, 5.40; N, 7.47.

Results and Discussion

Luminescence Data Treatment. The following relationship exists between the observed rate constant of Eu³⁺, k_{obsd} , and the mole fraction of H₂O in the solvent, $X_{\text{H}_2\text{O}}$: $k_{\text{obsd}} = k_{\text{nat}} + k_{\text{nonrad}} + k_{\text{H}_2\text{O}}X_{\text{H}_2\text{O}}$, where k_{nat} is the natural radiative decay constant, assuming that luminescence is the only deexcitation pathway; k_{nonrad} is the rate constant for all nonradiative deexcitation processes other than H₂O; $k_{\text{H}_2\text{O}}$ is the rate constant for deexcitation by OH vibrations of coordinated H₂O. Thus, the following equations can be written:

$$k_{\text{obsd}}\text{H}_2\text{O} = k_{\text{nat}} + k_{\text{nonrad}} + k_{\text{H}_2\text{O}} \quad (1)$$

$$k_{\text{obsd}}\text{D}_2\text{O} = k_{\text{nat}} + k_{\text{nonrad}} \quad (2)$$

$$\Delta k = k_{\text{obsd}}\text{H}_2\text{O} - k_{\text{obsd}}\text{D}_2\text{O} = k_{\text{H}_2\text{O}} \quad (3)$$

where $k_{\text{obsd}}\text{H}_2\text{O}$ is the observed rate constant of deexcitation in 100% H₂O ($X_{\text{H}_2\text{O}} = 1$) and $k_{\text{obsd}}\text{D}_2\text{O}$ is the observed rate constant of deexcitation in 100% D₂O ($X_{\text{H}_2\text{O}} = 0$).

Plots of rate constant for luminescence decay, k , vs. mole fraction of H₂O, $X_{\text{H}_2\text{O}}$, were constructed for aquo-Eu³⁺ and Eu³⁺ in solution with the three peptides Z-D-Gla-D-Gla-OMe, Z-L-Gla-L-Ser-OMe, and Z-Gly-D,L-Gla-Gly-OEt. In order to minimize error due to H₂O contamination at higher D₂O concentration, k was determined for each of these peptides at mole fractions of H₂O from 1.0 to 0.4. The k vs. $X_{\text{H}_2\text{O}}$ plots (Figure 1), which were all linear, were then extrapolated to the left-hand ordinate, or k axis, in order to obtain k for the peptides in 100% D₂O. The k -axis intercepts for all of the peptides were approximately equal, indicating that no dynamic quenching mechanism for the excited-state Eu³⁺ ion was introduced by the binding of peptide since such a process would increase the value of k_{nonrad} resulting in a shift of the k -axis intercept ($k_{\text{obsd}}\text{D}_2\text{O}$). Thus the observed changes in the luminescence decay constant result solely from variation in the number of water molecules surrounding the Eu³⁺ ion. The

principal features of interest in these plots of k vs. $X_{\text{H}_2\text{O}}$, then, are the values along the right-hand ordinates, i.e., the number of H_2O molecules (N) in the primary coordination sphere of Eu^{3+} .

In order to establish N along the right-hand axis, we compared our data to the work of Horrocks and Sudnick.⁷ Horrocks and Sudnick⁷ plotted the quantity Δk vs. N for a variety of crystalline Eu^{3+} complexes for which N had been determined from crystallographic data. The plot was linear and agreed well with the solution data. If we compare our value of 8.3 for Δk of aquo- Eu^{3+} to the plot of Δk vs. N constructed by Horrocks and Sudnick,⁷ our data fit closest with $N = 9$ for the Eu^{3+} aquo ion. Other references in the literature support the assumption that Ln^{3+} aquo ions are nonhydrated.¹²⁻¹⁵ The value $k_{\text{obsd}}^{\text{H}_2\text{O}}$ for aquo- Eu^{3+} was used to establish a point on the right-hand ($X_{\text{H}_2\text{O}} = 1$) ordinate, representing $N = 9.0$ in the plots of Figure 1. Since the k intercepts for aquo- Eu^{3+} and the three peptide: Eu^{3+} complexes were approximately equivalent, this value was used to determine the $N = 0.0$ point on the right-hand ordinate. A scale from 0.0 to 9.0 coordinated water molecules was then constructed along this axis to represent N , in accordance with method of Horrocks et al.⁸ A value of about $0.5\text{H}_2\text{O}$ is the probable uncertainty of these measurements. A quantity derived from estimates of N , ΔN , is defined as $N(\text{aquo-Eu}^{3+}) - N(\text{ligand-Eu}^{3+} \text{ complex})$, and can be interpreted as the number of H_2O molecules displaced from the coordination sphere of the Eu^{3+} ion by ligand complexation.

The observed value of the rate constant, k_{obsd} , is actually a weighted average of the k values of all Eu^{3+} species present in the mixture since the exchange rates of species in the primary coordination sphere of Eu^{3+} ions (10^8 – 10^4 s^{-1}) are far larger than the measured rates of deexcitation (10^2 – 10^4 s^{-1}). The following equation for k_{obsd} can be written:

$$k_{\text{obsd}} = k_{\text{F}}X_{\text{F}} + \sum_{i=1}^n k_{\text{B}_i}X_{\text{B}_i} \quad (4)$$

where k_{F} is the rate constant for aquo- Eu^{3+} , X_{F} is the fraction of unbound (aquo) Eu^{3+} , k_{B_i} is the rate constant for bound Eu^{3+} bound as species i , and X_{B_i} is the fraction of Eu^{3+} bound as species i . Further verification of our technique and system was obtained by investigation of the formation of $\text{EDTA}\cdot\text{Eu}^{3+}$ complexes at a variety of $X_{\text{H}_2\text{O}}$ values and concentration ratios of EDTA and Eu^{3+} ions. Our results were again in close agreement with those of Horrocks et al.⁸

The plots of $X_{\text{H}_2\text{O}}$ vs. k and N for the three peptides in Figure 1 show that the number of water molecules displaced from Eu^{3+} ions by these peptides is dependent on both the pH and on the formal concentration ratio of peptide to Eu^{3+} in the solution. These dependences were further investigated by peptide titrations into a solution of Eu^{3+} ions and by pH titrations of solutions containing peptide and Eu^{3+} .

Two of the four peptides studied, Z-L-Gla-L-Ser-OME and Z-Gly-D,L-Gla-Gly-OEt, precipitated out of solution to some degree when in solution with europium ions at pH values higher than 4.5–5.0. The precipitates remained uniformly suspended in the solution during the course of a luminescence decay measurement and did not appear to affect luminescence decay measurements as evidenced by the following observations: (1) No change in luminescence intensity was noted when precipitation occurred. (2) The results yielded smooth, monotonic curves through the point at which precipitation occurred. (3) As noted above, Horrocks and Sudnick⁷ found good agreement between luminescence decay constants measured on solids and in solution. No precipitation of europium hydroxide at pH values between 6 and 8 was observed for aquo- Eu^{3+} at concentration of 1 mM or less, although at higher concentration ($1 \times 10^{-2} \text{ M}$ and above) significant precipitation was observed as the pH was adjusted above 5.5. No change in rate constant

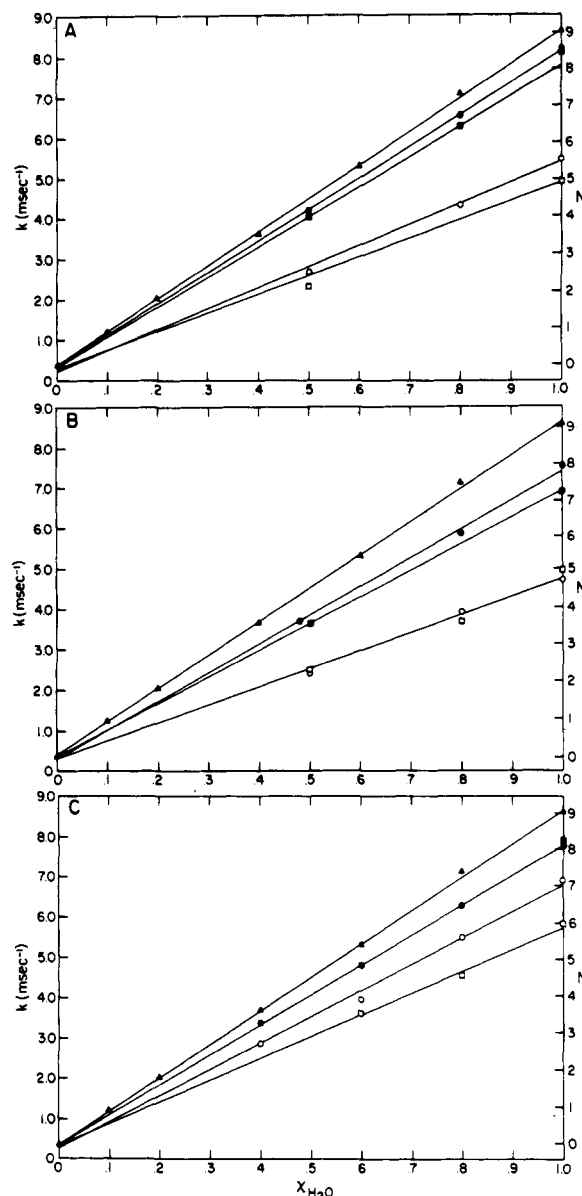


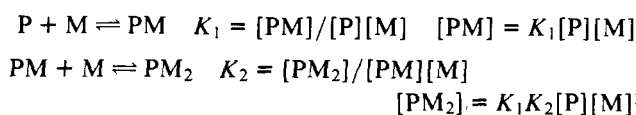
Figure 1. Effect of varying the molar ratio of H_2O in an $\text{H}_2\text{O}/\text{D}_2\text{O}$ solvent system on Eu^{3+} binding to Glu-containing peptides. (A) Z-Gly-D,L-Gla-Gly-OEt (XV): \blacktriangle aquo EuCl_3 , pH 5.8; \bullet 1:1 peptide: Eu^{3+} , pH 3.7; \blacksquare 2:1 peptide: Eu^{3+} , pH 3.5; \circ 1:1 peptide: Eu^{3+} , pH 6.3; \square 2:1 peptide: Eu^{3+} , pH 6.2. (B) Z-D-Gla-D-Gla-OME (III): \blacktriangle aquo EuCl_3 , pH 5.8; \bullet 1:1 peptide: Eu^{3+} , pH 3.2; \blacksquare 2:1 peptide: Eu^{3+} , pH 3.3; \circ 1:1 peptide: Eu^{3+} , pH 7.7; \square 2:1 peptide: Eu^{3+} , pH 7.8. (C) Z-L-Gla-L-Ser-OME (IV): \blacktriangle aquo- EuCl_3 , pH 5.8; \bullet 1:1 peptide: Eu^{3+} , pH 3.5; \blacksquare 2:1 peptide: Eu^{3+} , pH 3.4; \circ 1:1 peptide: Eu^{3+} , pH 6.2; \square 2:1 peptide: Eu^{3+} , pH 5.8.

or luminescence intensity for 1×10^{-3} and $1 \times 10^{-4} \text{ M}$ aquo- Eu^{3+} was observed over a pH range of 3.0–7.9.

Thermodynamic Equilibrium Analysis. To extract binding constants from the data for the peptide titration experiments (Figures 2 and 3), three thermodynamic equilibrium models were applied to each of the peptides.

The first model involves a maximum stoichiometry of two metal ions bound to one peptide molecule (2M:1P) and is defined by the following series of equilibrium reactions:

model 1
(2M:1P)



A quantity, r , the ratio of moles of bound metal to total moles

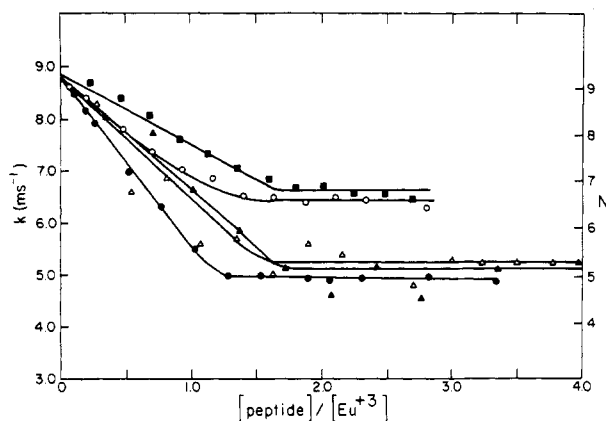


Figure 2. Peptide titrations of 1×10^{-3} M EuCl_3 : ■ free Gla, pH 7.8; ○ L-Phe-L-Leu-L-Gla-L-Glu-L-Leu-OMe (X), pH 7.0; ▲ Z-Gly-D,L-Gla-Gly-OEt (XV), pH 6.7; △ Z-L-Gla-L-Ser-OMe (IV), pH 6.8; ● L-Phe-L-Leu-L-Gla-L-Gla-L-Leu-OMe (XIV), pH 7.5.

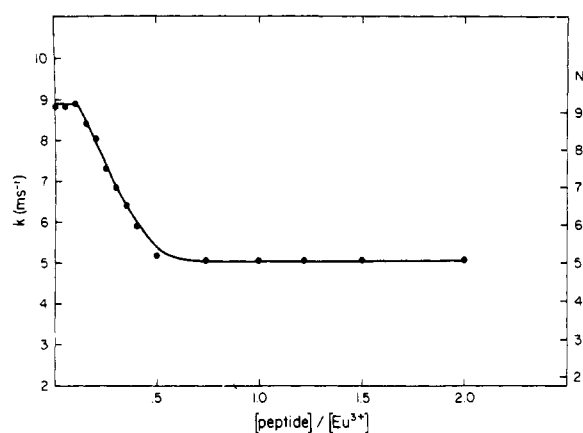


Figure 3. Z-D-Gla-D-Gla-OMe (III) titration of 1×10^{-4} M EuCl_3 , pH 7.5.

of peptide, is derived from the model above:

$$r = \frac{K_1[M] + 2K_1K_2[M]^2}{1 + K_1[M] + K_1K_2[M]^2} \quad (5a)$$

Equation 5a can be rearranged to give

$$r/[M] = K_1(1 - r) + K_1K_2[M](2 - r) \quad (5b)$$

The ratio r can be represented in terms of quantities determined by the data as

$$r = X_M[M]_T/[P]_T \quad (6)$$

X_M = fraction of metal bound

$[M]_T$ = total metal concentration

$[P]_T$ = total peptide concentration

The unbound metal ion concentration, $[M]$, is written as

$$[M] = (1 - X_M)[M]_T \quad (7)$$

Substituting eq 6 and 7 into (5b) and rearranging gives the following relationship:

$$X_M/(1 - X_M) = K_1([P]_T - X_M[M]_T) + K_1K_2[M]_T(1 - X_M)(2[P]_T - X_M[M]_T) \quad (8)$$

A function of X_M , $F(X_M)$, is defined by the left side of eq 8:

$$F(X_M) = X_M/(1 - X_M) \quad (9)$$

Rearrangement of eq 8 gives the following cubic equation in X_M :

$$K_1K_2[M]_T^2X_M^3 - X_M^2(K_1[M]_T + 2K_1K_2[M]_T^2 + 2K_1K_2[M]_T[P]_T) + X_M(K_1[M]_T + K_1[P]_T + K_1K_2[M]_T^2 + 4K_1K_2[M]_T[P]_T + 1) - K_1[P]_T - 2K_1K_2[M]_T[P]_T = 0 \quad (10)$$

The second model allows a maximum stoichiometry of one metal ion bound to a single peptide molecule (1M:1P):

model 2
(1M:1P)



The derivations are equivalent to those for model 1 with $K_2 = 0$. Equation 10 then simplifies to a quadratic in X_M .

The third model involves a maximum stoichiometry of the two peptide molecules bound to a single metal ion (1M:2P) and is defined as follows:

model 3
(1M:2P)



$$[P_2M] = K_1K_2[P]^2[M]$$

Two equations can be set up for the quantities X_P (fraction of peptide bound) and X_M (fraction of metal bound):

$$X_P = \frac{K_1[M][P] + 2K_1K_2[M][P]^2}{[P]_T} \quad (11a)$$

$$X_M = \frac{K_1[M][P] + K_1K_2[M][P]^2}{[M]_T} \quad (11b)$$

By subtracting the two equations (11a) and (11b) in order to eliminate the term $[P]^2$ and using the following relationship for X_P :

$$X_P = \frac{[P]_T - [P]}{[P]_T} \quad (12)$$

an expression for $[P]$ in terms of X_M is obtained:

$$[P] = \frac{2[M]_TX_M - [P]_T}{K_1[M] - 1} \quad (13)$$

Substitution of eq 13 and 7 into (11b) yields a cubic equation in X_M :

$$X_M^3(4K_1K_2[M]_T^2 - K_1^2[M]_T^2) - X_M^2(4K_1K_2[M]_T^2 + 4K_1K_2[M]_T[P]_T - 2K_1^2[M]_T^2 - K_1^2[M]_T[P]_T) + X_M(1 - K_1^2[M]_T^2 + K_1[P]_T + 4K_1K_2[M]_T[P]_T + K_1K_2[P]_T^2 - 2K_1^2[P]_T[M]_T) + K_1^2[P]_T[M]_T - K_1[P]_T - K_1K_2[P]_T^2 = 0 \quad (14)$$

An alternate derivation for this model is listed in the Appendix. Both derivations gave equivalent results in the analysis.

Experimental values for X_M can be estimated from the data for the peptide titrations (Figures 2 and 3) by using eq 4 and making the approximation that the product X_BK_B for one bound species of Eu^{3+} dominates the sum. The value of the rate constant at the level portion of the titration curve is then taken to be the rate constant for this bound species and X_M is calculated from the following rearrangement of eq 4.

$$X_M = (k_F - k_{\text{obsd}})/(k_F - k_B) \quad (15)$$

where k_B is the rate constant defined by the level portion of the titration curve and k_F and k_{obsd} are as previously defined. This approximation is always valid for model 2 (1M:1P) and is valid for models 1 (2M:1P) and 3 (1M:2P) if either of the following two conditions are satisfied: (1) $[MP] \ll [M_2P]$ for model 1 (2M:1P) or $[MP] \ll [MP_2]$ for model 3 (1M:2P); (2) k_B , (the rate constant for Eu^{3+} bound in the 1:1 complex) is approxi-

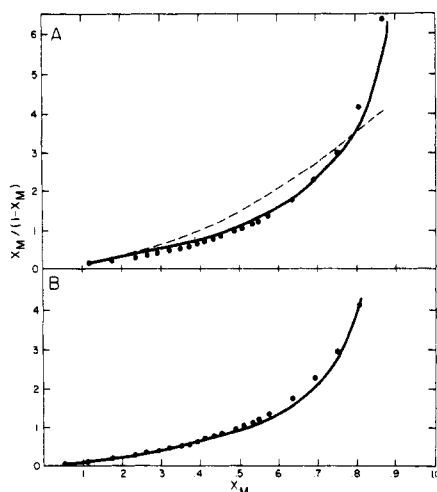


Figure 4. Nonlinear least-squares analysis of Z-Gly-D,L-Gla-Gly-OEt (XV). (A) ● experimental (from data in figure 2); — theoretical fit with model 3(1M:2P), $K_1^d = 5.9 \mu\text{M}$ and $K_2^d = 1.5 \mu\text{M}$; - - - theoretical fit with model 2(1M:1P), $K^d = 125 \mu\text{M}$. (B) ● experimental (from data in Figure 2); — theoretical fit with model 3(1M:2P), $K_1^d = 9 \text{ mM}$ and $K_2^d = 67 \mu\text{M}$.

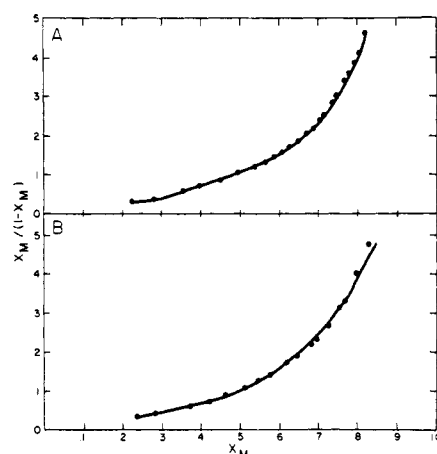


Figure 5. Nonlinear least-squares analysis. (A) L-Phe-L-Leu-L-Gla-L-Glu-L-Leu-OMe (X): ● experimental (from data in Figure 2); — theoretical fit with model 2(1M:1P), $K^d = 4.3 \mu\text{M}$. (B) L-Phe-L-Leu-L-Gla-L-Glu-L-Leu-OMe (XIV): ● experimental (from data in Figure 2); — theoretical fit with model 2(1M:1P), $K^d = 4.1 \mu\text{M}$.

mately equal to k_{B_2} (the rate constant for Eu^{3+} bound in the 2:1 complex).

For each peptide data set, a series of experimental values for the function defined by eq 9, $F(X_m)_{\text{exp}}$, can then be calculated.

A nonlinear least-squares computer analysis was used to obtain K_1 and K_2 (or in the case of model 2 K_1). The procedure for models 1 and 3 was to make an initial guess to K_1 and K_2 and set up a grid of values for K_1 and K_2 around the initial guess. At each point in the grid, eq 10 for model 1 or eq 14 for model 3 was solved for X_m over a range of values for P_T and a theoretical function, $F(X_m)_{\text{theor}}$, was calculated from eq 9. The function

$$S = \sum_{i=1}^n w_i [F(X_m)_{\text{exp}} - F(X_m)_{\text{theor}}]_i^2 \quad (16)$$

was minimized over the grid and the value of K_1 and K_2 at the minimum selected. A similar analysis was carried out for model 2 using eq 10 with $K_2 = 0$ to solve for X_m . The values chosen for K_1 and K_2 in the grid searches were in a range from 0 to 1×10^8 .

The above thermodynamic treatment supersedes an earlier simpler approach;¹¹ the results reported here are substantially

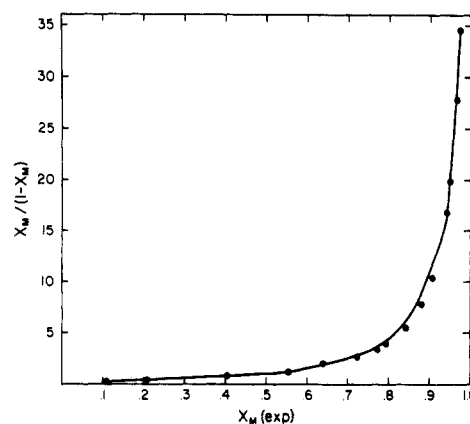


Figure 6. Nonlinear least-squares analysis of Z-D-Gla-D-Gla-OMe (III): ● experimental (from data in Figure 3); — theoretical fit with model 1(2M:1P), $K_1^d = 0.6 \mu\text{M}$ and $K_2^d = 1.1 \mu\text{M}$.

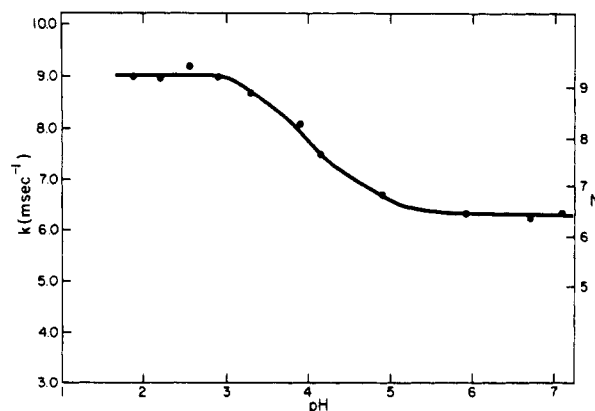


Figure 7. pH dependence of Eu^{3+} binding to L-Phe-L-Leu-L-Gla-L-Glu-L-Leu-OMe (X); formal ratio of peptide: Eu^{3+} was 2:1.

changed for several of the peptides from preliminary results previously reported.¹¹

Metal Ion Complexation. Europium(III):amino acid and metal ion:peptide titrations were carried out. The europium ion luminescence lifetime was the observed variable. In order to establish the composition of the metal ion complexes involved, nonlinear least-squares analyses of the data in terms of the three models developed in the Materials and Methods and Appendix sections were carried out (Figures 4–6, Table I). In each plot the ordinate represents $F(X_m)$ (eq 9) and the abscissa is the experimental value of X_m . Both $F(X_m)_{\text{exp}}$ (closed circles) and $F(X_m)_{\text{theor}}$ (solid and dashed lines) are plotted.

The zwitterionic form of the amino acid, Gla, was examined by these methods. The best fit was obtained with model 3 (1 Eu^{3+} :2 amino acid) with $K_1^d = 33 \mu\text{M}$ and $K_2^d = 5.9 \mu\text{M}$ (not shown), where K_1^d and K_2^d represent the reciprocals of the corresponding association constants. In a study involving energy transfer from Gla to the Tb^{3+} ion, Sperling et al.⁹ have reported $K^d = 55 \pm 15 \mu\text{M}$ and a stoichiometry of 2.1Gla bound per Tb^{3+} ion. These constants were based upon a Weber-Young¹¹ analysis of the experimental data. Such a treatment, however, is applicable only to noninteracting systems which contain equivalent metal ion binding sites and a single dissociation constant. It is unlikely that these conditions will be met in the interaction of a small, highly charged molecule, such as Gla, with metal ions. Thus, the more general thermodynamic treatment employed here which yields an excellent fit to the experimental data is likely to be more appropriate. Titration of europium ions with Gla (Figure 2) exhibits a constant value of $\Delta N = 2.2$ above a Gla: Eu^{3+} formal ratio of 1.6.

Table I. Parameters Characterizing Peptide:Eu³⁺ Complexes

peptide	ΔN^a	pH midpoint ^b	model ^c	$K_1^{d,d}$	$K_2^{d,d}$
Gla	2.2		3(1M:2P)	33 μ M	5.9 μ M
Z-Gly-D,L-Gla-Gly-OEt (XV)	3.9		3(1M:2P)	5.9 μ M 9.0 mM ^e	1.5 μ M 67.0 μ M
Phe-L-Leu-L-Gla-L-Gla-L-Leu-OMe (XIV)	4.0	3.7	2(1M:1P)	4.1 μ M	
Phe-L-Leu-L-Gla-L-Glu-L-Leu-OMe (X)	2.4	4.1	2(1M:1P)	4.3 μ M	
Z-L-Gla-L-Ser-OMe (IV)	3.7	4.8	3(1M:2P)	9.1 μ M 13.1 mM ^e	20.0 μ M 2.5 μ M
Z-D-Gla-D-Gla-OMe (III)	3.9	3.7	1(2M:1P)	0.6 μ M	1.1 μ M

^a ΔN = number of H₂O molecules displaced from the Eu³⁺ ion coordination sphere by ligand complexation. ^b pH midpoints are taken from the pH titration curves (Figures 9–12). ^c Model = equilibrium thermodynamic treatment assuming model 1 (2M:1P), model 2 (1M:1P), or model 3(1M:2P) where M = metal (Eu³⁺) and P = peptide. ^d $K_1^{d,d}$ and $K_2^{d,d}$ are the first and second dissociation constants obtained by nonlinear least-squares analysis of the data using the models in footnote c. ^e Two minima were obtained by the nonlinear least-squares analysis of model 3. The set of dissociation constants with $K_1^{d,d} = 9$ mM for Z-Gly-Gla-Gla-OEt and $K_2^{d,d} = 13.1$ mM for Z-Gla-Ser-OMe are not consistent with the micromolar values for $K_1^{d,d}$ obtained for other peptides in the series so these sets were discarded. ^f A more rigorous analysis was carried out according to a modification of the method of Shapiro and Johnson¹⁴ on those peptides exhibiting 2M:1P and 1M:2P stoichiometries in which k_{B_1} and k_{B_2} (rate constants for the 1:1 and 2:1 complexes, respectively) were calculated as parameters. Both K_1 and K_2 were allowed to vary freely. Stoichiometries (models) determined by this method were in agreement with those presented in this table and the ΔN values in this table were found to be the values for the 2:1 complexes. However, for a given set of values for k_{B_1} and k_{B_2} , good fits to the data were obtained over a wide range of values for the equilibrium constants indicating that the equilibrium constants are not as reliably determined by either method as the stoichiometries and bound rate constants (ΔN values).

The zwitterionic form of γ -carboxyglutamic acid is not a good model of the behavior of protein-bound Gla. As a better approximation of the behavior of protein-bound Gla residues, the tripeptide *N*-carbobenzylxyglycyl-D,L- γ -carboxyglutamylglycine ethyl ester (XV)¹⁰ was employed. The stoichiometric titration curve for this tripeptide, containing a single Gla residue (Figure 2), yields a constant value of $\Delta N = 3.9$ above a peptide:Eu³⁺ formal ratio of 1.7. The best fit to the data was obtained from the nonlinear least-squares analysis using model 3 (1Eu³⁺:2 peptide) (Figure 4A,B, solid lines). Model 2 (1Eu³⁺:1 peptide) (Figure 4A, dashed line) deviates sharply when $F(X_m)_{\text{theor}}$ is plotted against the experimental value of X_m . Good fits to the data were obtained from two different sets of K_1 and K_2 values (Table I). However, the extremely large value of $K_1^{d,d} = 9$ mM for the set of dissociation constants used to generate the solid line in Figure 4B is not consistent with the micromolar values obtained for the first dissociation constants of the metal ion complexes of the two pentapeptides (XIV, X) and free Gla. Based on the results for the other peptides and Gla, we conclude that the set of dissociation constants with $K_1^{d,d} = 5.9$ μ M and $K_2^{d,d} = 1.5$ μ M (Figure 4A, solid line) characterizes the interaction of Eu³⁺ with XV.

Since protein-bound Gla residues frequently occur in pairs, it is of importance to examine peptides of this type. The ligand titration curve (Figure 2) for the pentapeptide H-Phe-Leu-Gla-Gla-Leu-OMe (XIV) yields a constant value of $\Delta N = 4$ above a peptide:Eu³⁺ formal ratio of 1.3. A nonlinear least-squares analysis of the data (Figure 5B, solid curve) yielded a good fit with model 2 (1Eu³⁺:1 peptide) with a $K_1^{d,d} = 4.1$ μ M. A fit was also obtained with model 3 (1Eu³⁺:2 peptide) with $K_1^{d,d} = 4.0$ μ M and $K_2^{d,d} = 5.0$ mM indicating formation of the 1:1 complex as the predominant species with small amounts of the 2:1 peptide:Eu³⁺ complex present. A simpler peptide containing two adjacent Gla moieties, Z-D-Gla-D-Gla-OMe (III), was employed to titrate Eu³⁺. The titration curve (Figure 3) leveled off at a 0.5:1 peptide:metal ion formal ratio with a ΔN of 3.9. The nonlinear least-squares analysis of this data (Figure 6, solid line) yielded an excellent fit with model 1 (2Eu³⁺:1 peptide) with $K_1^{d,d} = 0.6$ μ M and $K_2^{d,d} = 1.1$ μ M. Thus, it appears that two adjacent Gla residues are capable of binding two Eu³⁺ ions with extremely high association constants. However, residues bounding the -Gla-Gla- pair have a profound effect on the ability of the second metal ion to bind. The addition of the Phe-Leu pair on the amino terminus and Leu on the carboxy terminus of -Gla-Gla- to yield pentapeptide

XIV results in the formation of a 1:1 complex with Eu³⁺ ions with a weaker dissociation constant. The leucine residues either by virtue of their size or hydrophobic character may inhibit the binding of a second Eu³⁺ ion. On the other hand, the structure of this pentapeptide also allows the possibility of intramolecular hydrogen bonding between the free amino terminus and Gla γ -carboxyl groups which could similarly hinder the formation of a 2:1 Eu³⁺:XIV complex.

In order to compare the results obtained with III and XIV to peptides containing Gla and some other adjacent residue with an oxygen ligand the pentapeptide H-Phe-Leu-Gla-Glu-Leu-OMe (X) and the dipeptide Z-Gla-Ser-OMe (IV) were examined. The curve obtained by titration of Eu³⁺ with X (Figure 2) leveled off above a 1.4 formal ratio of peptide:Eu³⁺ at a ΔN value of 2.4. The nonlinear least-squares analysis yielded an excellent fit to this data with model 2 (1Eu³⁺:1 peptide), $K_1^{d,d} = 4.3$ μ M (Figure 5A, solid line). Good fits were also obtained when models 1 and 3 were plotted; large values of $K_2^{d,d}$ in the millimolar range resulted (10 and 0.7 mM, respectively) with the same value of $K_1^{d,d} = 4.3$ μ M in each case. These results suggest that, as with XIV, the pentapeptide X also forms a 1:1 peptide:Eu³⁺ complex with the coexistence of small amounts of 1:2 and 2:1 peptide:Eu³⁺ complexes.

Examination of the interaction of IV with Eu³⁺ (Figure 2) indicated a constant value of $\Delta N = 3.7$ above a formal ratio of 1.7:1 peptide to Eu³⁺. The results of the nonlinear least-squares analysis again yielded two distinct minima with widely differing values of K_1 and K_2 (Table I). The theoretical function $F(X_m)_{\text{theor}}$ generated with values of $K_1^{d,d} = 13.1$ mM and $K_2^{d,d} = 2.5$ μ M (not shown) had a curve shape which differed from both the experimental curve and from all other curves generated in the analysis of this peptide series. That is, the curve did not smoothly decrease with X_m but assumed an irregular shape near $X_m = 0.06$. The questionable behavior of this function tends to limit it as a possible model for IV. Also, as for XV, the value of $K_1^{d,d} = 13.1$ mM is not consistent with the results for the other peptides which yielded first dissociation constants on the order of micromolar. The second set of constants, $K_1^{d,d} = 9.1$ μ M and $K_2^{d,d} = 20$ μ M, model 3 (1M:2P), consistent with those for the other peptides and the theoretical function generated by them, is well behaved. Thus, this set was selected as better characterizing the interaction of IV with Eu³⁺ ions. The behavior of IV is similar to the interactions observed with Z-Gly-D,L-Gla-Gly-OEt and Eu³⁺ (Table I), although the contribution of the serine hydroxyl as a pathway for radiationless deexcitation of the europium ion may be

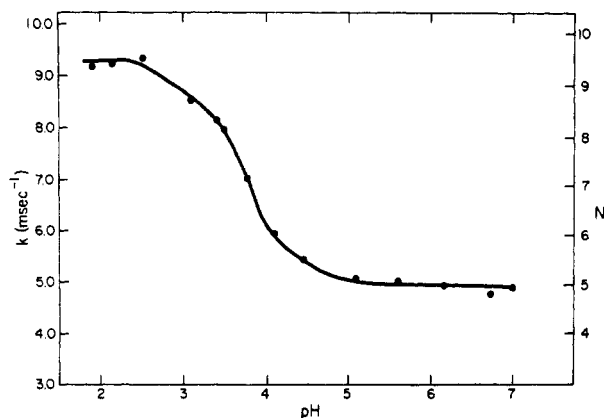


Figure 8. pH dependence of Eu^{3+} binding to L-Phe-L-Leu-L-Gla-L-Gla-L-Leu-OMe (XIV); formal ratio of peptide: Eu^{3+} was 2:1.

present but not observed in the determined value of ΔN . Haas and Stein¹³ have reported that the hydroxyl group of methanol can quench europium luminescence, although not as efficiently as water.

In terms of the number of water molecules displaced from the europium(III) ion coordination sphere as a result of ligand complexation, two distinct types of behavior were observed in the peptide series reported here. Results for peptides IV, X, XIV, and XV suggest a model in which a single peptide-bound Gla residue will interact with Eu^{3+} with an overall loss of approximately two molecules of water from the metal ion. A peptide: Eu^{3+} complex of 2:1 is preferred for peptides containing single Gla residues (IV and XV). Such complexes are consistent with the above model. Peptides with either a Gla or Glu residue adjacent to Gla form 1:1 complexes with ΔN values consistent with the model. The metal ion binding behavior of III illustrates the second type of Eu^{3+} coordination which involves the formation of a 2:1 Eu^{3+} :peptide complex and ΔN value which indicates the displacement of four water molecules from the coordination sphere of each of the two bound Eu^{3+} ions.

The ΔN value of 2.2 observed for the 2:1 fully deblocked Gla: Eu^{3+} complex is not consistent with the behavior described above and with the model proposed by Sperling et al.⁹ Compared with Gly-Gla-Gly (XV), unblocked Gla binds Eu^{3+} significantly less tightly. As a result of these observations and those reported by Sperling et al.,⁹ a model of the ternary Eu^{3+} :2Gla complex can be developed which retains the symmetry of placement of the lanthanide ion with respect to the Gla γ carbon and the carboxyl groups required by Sperling et al. In each Gla molecule, the free α -amino group of unblocked Gla may be visualized as interacting with one γ -carboxyl group, rendering it essentially unavailable for interaction with the Eu^{3+} ion. Furthermore, the free γ -carboxyl group in each Gla appears not to be involved in complexation with the Eu^{3+} ion. Thus, only one γ -carboxyl group in each Gla appears to be involved in complexation with the Eu^{3+} ion with the displacement of approximately one water molecule per free Gla.

pH Titrations. At approximately 20 mM metal ion concentrations the pH dependence of calcium and magnesium ion binding to bovine prothrombin fragment 1 yields apparent pK_a values of 3.8 and 4.3, respectively.⁶ In order to correlate the behavior of Eu^{3+} binding to prothrombin fragment 1 and the pH dependence of that binding we have examined the pH dependence of the binding of Eu^{3+} to Gla-containing peptides. Such studies may ultimately suggest those ionizable side chain groups that are involved in the fragment 1: Eu^{3+} interaction. The pH titration of a 2:1 XIV: Eu^{3+} formal ratio (Figure 8) yielded a sigmoidal curve with a midpoint at pH 3.7; the curve leveled off above pH 5.0 at a ΔN value of 4. In contrast the

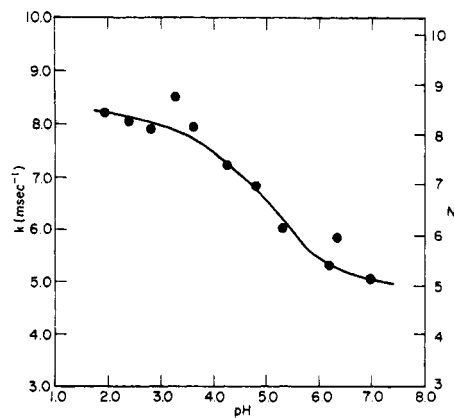


Figure 9. pH dependence of Eu^{3+} binding to Z-L-Gla-L-Ser-OMe (IV); formal ratio of peptide: Eu^{3+} was 2:1.

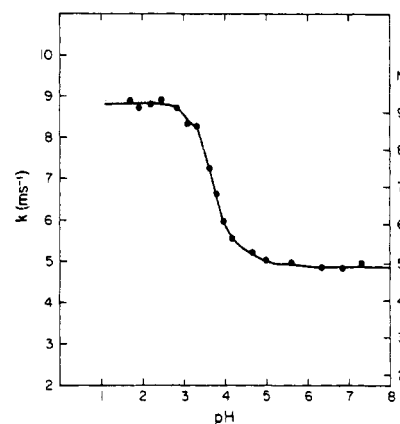


Figure 10. pH dependence of Eu^{3+} binding to Z-D-Gla-D-Gla-OMe (III); formal ratio of peptide: Eu^{3+} was 1.5:1.

Gla-Glu pentapeptide, X, yielded a sigmoidal curve (Figure 7) with a slightly higher midpoint, pH 4.1; the curve leveled off at pH 5.5 to a ΔN value of 2.5. The pH titration of a 1.5:1 III: Eu^{3+} formal ratio (Figure 10) resulted in a sigmoidal curve with a midpoint at pH 3.7. The curve leveled off above pH 5.0 at a ΔN of 4. The midpoint of the sigmoidal curve resulting from the titration of the Gla-Ser peptide IV (Figure 9) is pH 4.8. No pH titration was done for Z-Gly-D,L-Gla-Gly-OEt (XV); however, the rate constant for luminescence decay of Eu^{3+} was constant giving a ΔN value of 3.9 for a 1.5:1 XV: Eu^{3+} formal ratio over a pH range between 6.2 and 7.2. The results of these pH studies show that the midpoint of the sigmoidal titration curves has a marked dependence on the nature of the groups adjacent to Gla on the peptide. The resulting titration midpoints are consistent with the averages of the pK_a s of the involved ionizing groups.

Conclusions

The utilization of europium ion luminescence lifetime measurements has yielded two types of data both of which are crucial to the development of a detailed model describing Eu^{3+} complexation with a series of Gla-containing peptides. First, in the presence of excess peptide, the metal ion luminescence lifetime determined as a function of solvent composition yields the number of water molecules displaced upon complexation. Thus, the number of involved ligands can be estimated to be equal to the number of waters displaced with the potential exception of the Gla-Ser peptide noted above. Second, analysis of the Eu^{3+} -peptide titration curves at fixed pH yields binding constants and the complex stoichiometry. Stoichiometries of 1 metal:1 peptide, 2 metal:1 peptide, and 1 metal:2 peptide were observed in this series and some of the forces dictating

complex structure are discussed. In addition, pH titrations of Eu^{3+} :peptide complexes yield information pertinent to the ionizing groups involved in Eu^{3+} complexation. Clearly, negatively charged oxygen atoms are involved, but the midpoints of the titration curves are shown in this series to vary by as much as a pH unit, depending on the detailed primary structure of the peptides.

Extension of these studies to larger Gla-containing peptides will potentially allow assessment of the role of secondary structure in the observed Eu^{3+} complexation behavior of Gla-containing proteins.

Acknowledgment. This investigation was supported by Grants HL 20161, HL 18245, and HL 23881 from the National Institutes of Health and by a grant from the North Carolina Science and Technology Committee. N.T.B. III was supported as a postdoctoral trainee, Grant HL 07255; K.A.K. was an Established Investigator of the American Heart Association. The laser laboratory facility at the University of North Carolina at Chapel Hill was established through the National Science Foundation (Grant CHEM 77-14547). The authors are particularly grateful to Professor W. Dew. Horrocks, Mr. D. R. Sudnick, and Mr. Al Schultz for their assistance in the early stages of this study. The technical assistance of Mr. W. S. Woodward is gratefully acknowledged.

Appendix. Alternate Derivation for Model 3

The following expressions are set up for X_p and X_m :

$$X_p = \frac{K_1[M] + 2K_1K_2[M][P]}{1 + K_1[M] + 2K_1K_2[M][P]} \quad (\text{A.1})$$

$$X_m = \frac{K_1[P] + K_1K_2[P]^2}{1 + K_1[P] + K_1K_2[P]^2} \quad (\text{A.2})$$

where $[P] = (1 - X_p)[P]_T$ and $[M] = (1 - X_m)[M]_T$. Solving eq A.1 for $[M]$, the following expression is obtained:

$$K_1[M](X_p + 2K_2[P]X_p - 2K_2[P] - 1) = -X_p \quad (\text{A.3})$$

Substituting (A.2) into (A.3) and rearranging the following

cubic in X_p is derived:

$$\begin{aligned} K_1K_2[P]_T^2X_p^3 - X_p^2(K_1[P]_T + 2K_1K_2[P]_T^2 \\ + 2K_1K_2[M]_T[P]_T) + X_p(K_1[P]_T + K_1K_2[P]_T^2 \\ + K_1[M]_T + 4K_1K_2[M]_T[P]_T + 1) \\ - 2K_1K_2[M]_T[P]_T - K_1[M]_T = 0 \quad (\text{A.4}) \end{aligned}$$

The procedure for the nonlinear least-squares analysis was to solve (A.4) for X_p at each value of K_1 and K_2 over a range of data values for $[P]_T$, then use (A.2) to solve for X_m .

References and Notes

- (1) (a) W. R. Kenan, Jr. Laboratories of Chemistry. (b) Department of Pathology.
- (2) (a) Stenflo, J.; Fernlund, P.; Egan, W.; Roepstorff, P. *Proc. Natl. Acad. Sci. U.S.A.* **1975**, *71*, 2730. (b) Nelsestuen, G. L.; Zytokovics, T. H.; Howard, J. B. *J. Biol. Chem.* **1974**, *249*, 6347.
- (3) Esmon, C. T.; Suttie, J. W.; Jackson, C. M. *J. Biol. Chem.* **1975**, *250*, 4095.
- (4) Hauschka, P. V.; Lian, J. B.; Gallop, P. M. *Proc. Natl. Acad. Sci. U.S.A.* **1975**, *72*, 1207. Price, P. A.; Otsuka, A. S.; Poser, J. W.; Kristaponis, J.; Raman, N. *Ibid.* **1979**, *73*, 1447.
- (5) Robertson, Jr., P.; Hiskey, R. G.; Koehler, K. A. *J. Biol. Chem.* **1978**, *253*, 5880.
- (6) Robertson, Jr., P.; Koehler, K. A.; Hiskey, R. G. *Biochem. Biophys. Res. Commun.* **1979**, *86*, 265.
- (7) Horrocks, Jr., W. DeW.; Sudnick, D. R. *J. Am. Chem. Soc.* **1979**, *101*, 334.
- (8) Horrocks, Jr., W. DeW.; Schmidt, G. F.; Sudnick, D. R.; Kittrell, C.; Bernheim, R. A. *J. Am. Chem. Soc.* **1977**, *99*, 2378.
- (9) Sperling, R.; Furie, B. C.; Blumenstein, M.; Keyt, B. *J. Biol. Chem.* **1978**, *253*, 3898.
- (10) Boggs, III, N. T.; Goldsmith, B.; Gawley, R. E.; Koehler, K. A.; Hiskey, R. G. *J. Org. Chem.* **1979**, *44*, 2262.
- (11) Marsh, H. C.; Boggs, N. T. III; Robertson, P., Jr.; Sarasua, M. M.; Scott, M. E.; Ten Kortenaar, P. B. W.; Helporn, J. A.; Pedersen, L. G.; Koehler, K. A.; Hiskey, R. G. In "Vitamin K. Metabolism and Vitamin K-Dependent Proteins", Suttie, J. W., Ed.; University Park Press: Baltimore, Md., 1979; p 137.
- (12) Weber, G.; Young, L. B. *J. Biol. Chem.* **1964**, *239*, 1415.
- (13) Haas, Y.; Stein, G. *J. Phys. Chem.* **1971**, *75*, 3677.
- (14) Reuben, J. *Biochemistry* **1971**, *10*, 2834.
- (15) Morgan, L. O. *J. Chem. Phys.* **1963**, *38*, 2788.
- (16) Grenthe, I.; Hessler, G.; Ots, H. *Acta Chem. Scand.* **1973**, *27*, 2543.
- (17) Sherry, A. D.; Yoshida, C.; Birnbaum, E. R.; Darnall, D. W. *J. Am. Chem. Soc.* **1973**, *95*, 3011.
- (18) Shapiro, B. L.; Johnston, M. D. *J. Am. Chem. Soc.* **1972**, *94*, 23.